JOURNAL OF CATALYSIS 147, 72–81 (1994)

Hydrogenation of Organic Oxygenates on Ni/Al_2O_3 and Ni/SiO_2 Catalysts

Baoshu Chen and John L. Falconer

Department of Chemical Engineering, University of Colorado, Boulder, Colorado 80309-0424

Received June 28, 1993; Revised December 21, 1993

Temperature-programmed reaction (TPR) was used to compare the hydrogenation rates of adsorbed methanol, ethanol, 1-propanol, dimethyl ether, formic acid, acetaldehyde, acetone, and methoxy (formed from coadsorbed CO and H_2) on a Ni/Al_2O_3 catalyst. The oxygenates adsorb on the Al_2O_3 support, and hydrogenation involves a spillover process since H_2 dissociates on the Ni surface. The rates of hydrogenation to CH_4 are essentially the same for all the oxygenates studied. Apparently the same rate-determining step, reverse spillover of an oxygenated species from Al_2O_3 to Ni, limits the formation of CH_4. Similar processes occur on Ni/SiO_2 for methanol and ethanol, but their coverages on SiO_2 are a factor of 15 lower and hydrogenation to CH_4 takes place over a broad temperature range. None of the oxygenates remained on the Ni surface of Ni/Al_2O_3 in H_2 flow; apparently they spilled over to the Al_2O_3 or were hydrogenated at room temperature. On Ni/SiO_2, only HCOOH adsorbs and dissociates on Ni to form adsorbed CO. Coadsorption shows that ^{13}CO and various oxygenates have independent adsorption and hydrogenation behavior. © 1994 Academic Press, Inc.

INTRODUCTION

Transient reaction studies, in which the adsorption steps are separated from the reaction and desorption steps, are particularly useful for understanding catalytic processes in which two reactants can adsorb on different phases of the catalyst surface. Such reaction process may involve spillover. For example, previous studies have used temperature-programmed reaction (TPR) on Ni/Al_2O_3 catalysts to study CO hydrogenation (1–7). Those studies showed that both CO and H_2 initially adsorbed on Ni, but CH_3O formed on the Al_2O_3 support by a spillover process. The CH_3O was hydrogenated during TPR in flowing H_2, which dissociated on the Ni surface. In the current study, hydrogenation of organic oxygenates on Ni/Al_2O_3 was studied by the same TPR procedure. The organic reactants were adsorbed directly on the Al_2O_3 support at room temperature, and H_2 was continuously supplied to the Ni surface as the catalyst temperature was ramped. Since the initial locations of the adsorbents are known, the rate of spillover must be as fast as the rate of product formation. TPR of a few of the organic reactants was also carried out on Al_2O_3 alone and on a Ni/SiO_2 catalyst. Alumina was used alone to show that the oxygenates adsorb directly on the Al_2O_3 support of Ni/Al_2O_3.

One interesting aspect of this study is that all the molecules studied hydrogenated to CH_4 on Ni/Al_2O_3 at essentially identical rates. That is, their rates of hydrogenation all appear limited by the same rate-determining step. Moreover, in most cases, the majority of the adsorbed organic reactant is hydrogenated to CH_4. Because the organics decompose at much higher temperatures on Al_2O_3 than the temperatures at which they hydrogenate to CH_4 on Ni/Al_2O_3, spillover is a critical step in the reaction process during TPR.

Methanol, ethanol, and propanol were used because they have all been reported to form alkoxides on Al_2O_3 surfaces (8–13). Similarly, $CO + H_2$ form CH_3O on the Al_2O_3 support of Ni/Al_2O_3. Since formates have been reported to form on Al_2O_3 from CO and H_2 under some conditions (14–17), formate was also formed by HCOOH adsorption (18–21), and the adsorbed formate was then hydrogenated during TPR. Since CH_3OH dehydrates on Al_2O_3 surfaces to form dimethyl ether, $(CH_3)_2O$ (22, 23), and $(CH_3)_2O$ has been reported to dissociate to form CH_3O on Al_2O_3 (24), TPR was also used to study $(CH_3)_2O$ hydrogenation. Formaldehyde, CH_2O, may be an intermediate as HCOO reacts to CH_3O on Al_2O_3 (25), and thus its hydrogenation behavior is also of interest. However, because CH_2O is a solid at room temperature and thus difficult to adsorb, acetaldehyde, C_2H_4O, was used instead. Acetone, $(CH_3)_2CO$, hydrogenation was studied by TPR because, like CO hydrogenation (26–28), the turnover frequency for acetone hydrogenation depends on the support (29).

All these organics adsorbed to high coverages on the Al_2O_3 surface of Ni/Al_2O_3 and they all hydrogenated to CH_4. In contrast, the amount of adsorption on the SiO_2 surface of Ni/SiO_2 was much smaller, and thus only a few organic reactants were studied by TPR on Ni/SiO_2. The

0021-9517/94 $6.00

competition between CO and organics for adsorption sites was studied for a few organics on both Ni/Al_2O_3 and Ni/SiO_2, and CO adsorption was not influenced by adsorption of the organic reactants.

EXPERIMENTAL METHODS

Temperature-programmed desorption (TPD) and reaction (TPR) experiments were carried out on Ni/Al_2O_3, Ni/SiO_2, and Al_2O_3 in a system that was described previously (2, 6). A 100-mg sample of the catalyst was supported on a frit in a quartz reactor, and the carrier gas (H_2 or He) at atmospheric pressure flowed over the catalyst at a flow rate of 100 cm^3/min (STP). Immediately downstream, the gas was analyzed with a UTI quadrupole mass spectrometer located in a turbopumped ultrahigh vacuum system. A computer system allowed simultaneous detection of multiple mass peaks. A 0.25-mm-diameter shielded thermocouple was connected to a derivative-proportional temperature programmer, which controlled an electric furnace to provide a constant heating rate of 1 K/s.

At the beginning of each series of experiments, the reduced and passivated catalyst was pretreated for 2 h at 773 K in ambient pressure H_2 flow. To maintain a clean surface, the catalyst was held in H_2 at 773 K for 10–15 min after each TPR experiment. Carbon monoxide (10% ^{12}CO/90% He, or ^{13}CO) and dimethyl ether were injected with a pulse valve into a He or H_2 carrier gas that continually flowed through the catalyst. The other oxygenates were injected slowly with a liquid syringe into the He carrier gas upstream to the reactor. The liquid accumulated on the tip of the syringe and then evaporated into the gas phase at room temperature.

After adsorption, the catalyst was held in H_2 at ambient temperature for 30 min for equilibration, and TPR was carried out by heating the catalyst in H_2 flow while detecting products with the mass spectrometer. For TPD experiments, the catalyst temperature was raised in He instead of H_2 flow. The cracking fractions at mass 15 from CH_3OH, HCOOH, and $(CH_3)_2O$ were subtracted from the mass 15 signals to obtain the CH_4 signals. Similarly, the signals at mass 28 were corrected for the cracking of CH_3OH, CO_2, C_2H_6, C_2H_4, $(CH_3)_2O$, and HCOOH to obtain the CO signals. When ^{13}CO was adsorbed, masses 17 ($^{13}CH_4$), 29 (^{13}CO), and 45 ($^{13}CO_2$) were also monitored during TPR. Mass 17 was corrected for H_2O cracking to obtain the $^{13}CH_4$ signal, and mass 15 was corrected for $^{13}CH_4$ cracking. Known volumes of pure gases or liquids were injected into the carrier gas, downstream of the reactor, to calibrate the mass spectrometer.

The catalysts (5.7% Ni/Al_2O_3 and 9.5% Ni/SiO_2) were prepared by impregnating Kaiser γ-Al_2O_3 (A-201) and Davison silica (Grade 57), respectively, to incipient wetness with an aqueous solution of nickel nitrate hydrate. After being dried in a vacuum oven for 24 h at 373–383 K, the catalysts were directly reduced in H_2 for 10 h at 773 K and passivated with 2% O_2 in N_2 at room temperature. Weight loadings were measured by atomic absorption. The dispersions of Ni on Ni/SiO_2 and Ni/Al_2O_3 are 2.4 and 1.7%, respectively, and were estimated from the amounts of CH_4 and CO observed during TPR for CO adsorption at 300 K. Kaiser γ-Al_2O_3 (A-201) was also used alone; its surface area is 220 m^2/g (30).

RESULTS

Nickel/Silica

Although CH_3O formed from CO + H_2 on Ni/Al_2O_3 catalysts (6, 31), it did not form on Ni/SiO_2 under the same conditions (31, 32). Instead, as shown in Fig. 1a, when CO was adsorbed at 300 K on the Ni surface of Ni/SiO_2, it reacted to form CH_4 in a single peak centered at 480 K (32, 33). The majority of the CO reacted to CH_4 (24 μmol/g catalyst), but 15 μmol CO/g catalyst desorbed between 300 and 500 K. When ^{12}CO was adsorbed at 300 K and then ^{13}CO was exposed to the catalyst at 300 K for 30 min, the ^{13}CO readily displaced ^{12}CO. During the subsequent TPR, only ^{13}CO and $^{13}CH_4$ were observed,

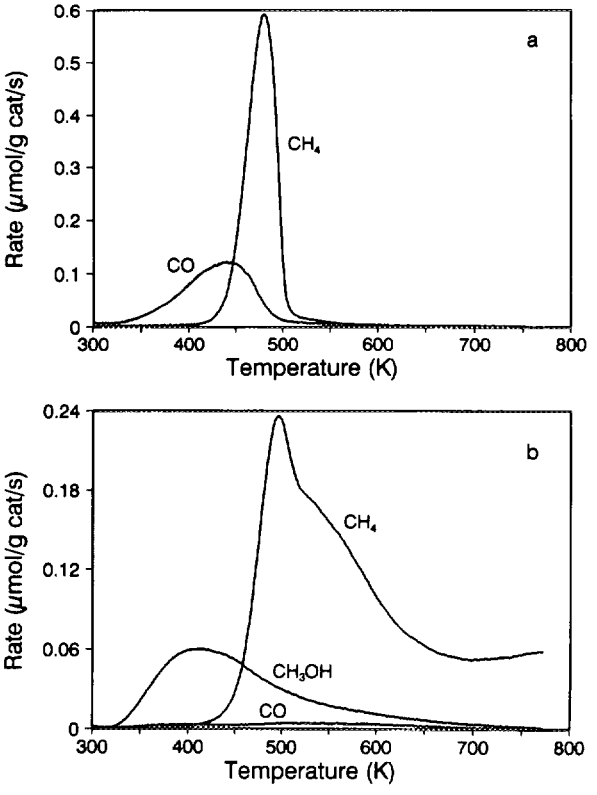

FIG. 1. TPR spectra on 9.5% Ni/SiO_2 following adsorption at 300 K of (a) CO for 15 min, (b) 4 μl CH_3OH.

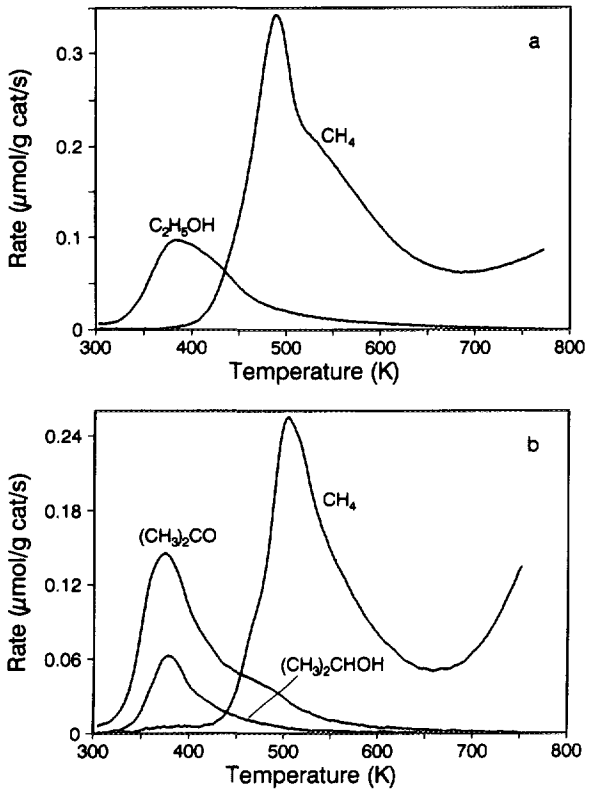

FIG. 2. TPR spectra on 9.5% Ni/SiO_2 following adsorption at 300 K of (a) 2 μl C_2H_5OH (b) 2 μl $(CH_3)_2CO$.

and these signals were identical to the corresponding signals in Fig. 1a.

The TPR spectra for CH_3OH adsorbed on Ni/SiO_2 at 300 K (Fig. 1b) indicate that CH_3OH did not decompose on the Ni surface and form CO during adsorption. Methane formed in a peak with a maximum at 495 K and in a broad peak that extended to 775 K; the CH_4 signal in Fig. 1b is quite different from that obtained for CO adsorption (Fig. 1a). For the high CH_3OH exposure used (1000 μmol/g catalyst), only 33 μmol CH_4/g catalyst was produced, and 11 μmol CH_3OH/g catalyst desorbed. To help identify adsorption sites, CH_3OH and ^{13}CO were sequentially adsorbed at 300 K, using the same exposures as in Figs. 1a and 1b. Isotope labeling allowed us to distinguish whether CH_4 formed from CO or CH_3OH. During the subsequent TPR, the ^{13}CO and $^{13}CH_4$ signals were similar to the corresponding signals in Fig. 1a, and the ^{12}CO and $^{12}CH_4$ signals were similar to the corresponding signals in Fig. 1b. The ^{13}C and ^{12}C product amounts were almost the same as the corresponding amounts in Figs. 1a and 1b. That is, ^{13}CO and $^{12}CH_3OH$ adsorbed independently of each other on Ni/SiO_2. The subsequent adsorption of ^{13}CO did not displace adsorbed CH_3OH, and the adsorbed CH_3OH did not block sites for ^{13}CO adsorption. Apparently, CH_3OH adsorbed on the SiO_2 support and did not form CO on the Ni surface.

Ethanol adsorption and hydrogenation on Ni/SiO_2 were quite similar to the same processes for CH_3OH. For high C_2H_5OH exposure (340 μmol/g catalyst), only 45 μmol CH_4 formed per gram of catalyst, and no other products besides unreacted C_2H_5OH were detected. Moreover, the CH_4 spectrum from C_2H_5OH hydrogenation (Fig. 2a) is almost identical in shape to CH_4 from CH_3OH hydrogenation. Both spectra consist of a narrow CH_4 peak, a broader peak at higher temperature, and CH_4 formation to 773 K, where heating was stopped. The only significant difference is that CH_4 from C_2H_5OH started forming at lower temperature.

The CH_4 TPR spectrum for $(CH_3)_2CO$ hydrogenation (Fig. 2b) was also similar to the CH_4 TPR spectrum for CH_3OH hydrogenation. Methane (35 μmol/g catalyst) started forming at 425 K and had a peak maximum at 504 K. The CH_4 rate was increasing significantly at 773 K, when heating was stopped to minimize catalyst sintering. Unreacted $(CH_3)_2CO$ desorbed in two peaks below 550 K, and some $(CH_3)_2CO$ was hydrogenated to $(CH_3)_2CHOH$ at low temperatures.

In contrast to the methane TPR spectra for CH_3OH, C_2H_5OH, and $(CH_3)_2CO$, the methane TPR spectrum of HCOOH on Ni/SiO_2 (Fig. 3) was almost identical to that obtained for adsorbed CO. Methane formed in a narrow peak centered at 486 K, and the only difference from CO hydrogenation was the presence of a small, high temperature tail. In addition to CH_4 (32 μmol/g catalyst), unreacted HCOOH desorbed below 450 K, and a significant amount of CO_2 (34 μmol/g catalyst) formed at the same time. A small amount of CO (9 μmol/g catalyst) also formed. The HCOOH exposure was 520 μmol/g catalyst.

Alumina

As reported previously (34), methanol, ethanol, and 1-propanol readily adsorb on Al_2O_3. When the Al_2O_3 temperature was raised in He flow (TPD) following CH_3OH

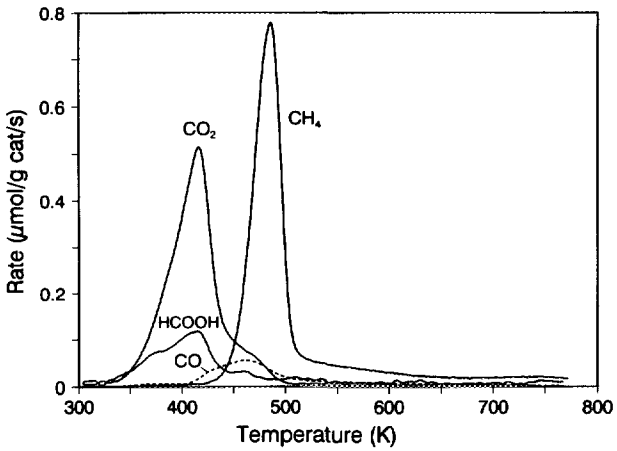

FIG. 3. TPR spectra on 9.5% Ni/SiO_2 following 2 μl of HCOOH exposure in He at 300 K.

adsorption, the majority of the CH_3OH decomposed above 700 K to form CO and H_2, as shown in Fig. 4a. Some CH_3OH dehydrated to dimethyl ether ($(CH_3)_2O$) and H_2O at lower temperature, and a small amount of unreacted CH_3OH desorbed. Three aspects of the methanol TPD spectra on Al_2O_3 are of interest for the TPR experiments on Ni/Al_2O_3:

- The 2 μL of CH_3OH (500 μmol/g catalyst) that was exposed to the Al_2O_3 readily adsorbed; it was all observed during TPD as decomposition products or unreacted CH_3OH.
- Using H_2 flow (TPR) instead of He flow (TPD) gave the same spectra as in Fig. 4a. Hydrogen desorption could not be observed during TPR, however, because of the high H_2 concentration in the gas stream. The gas phase H_2 had no influence on decomposition of adsorbed CH_3OH, apparently because H_2 does not dissociate on Al_2O_3.
- Methanol decomposed at much higher temperatures on Al_2O_3 than the temperatures at which it hydrogenated to CH_4 on Ni/Al_2O_3.

During TPD, C_2H_5OH and $1\text{-}C_3H_7OH$ decomposed more rapidly than CH_3OH on Al_2O_3, and their main reactions were dehydrogenation to C_2H_4 and C_3H_6, respectively. Dimethyl ether TPD spectra were similar to those obtained for CH_3OH TPD; most of the $(CH_3)_2O$ decomposed above 700 K to form CO and H_2 in single peaks at 780 K, and weakly adsorbed $(CH_3)_2O$ desorbed below 550 K. TPD results are reported in detail elsewhere (34).

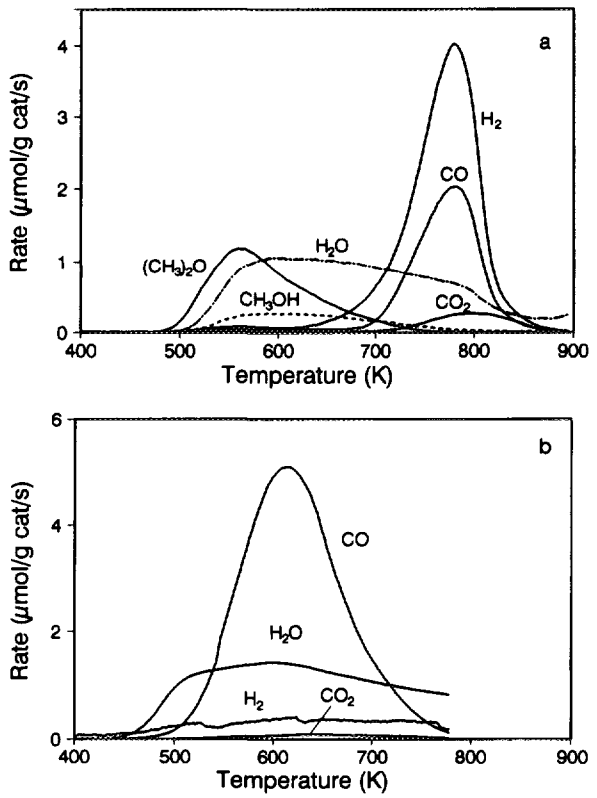

FIG. 4. TPD spectra on Al_2O_3 following adsorption at 300 K of (a) 2 μl CH_3OH, (b) 3 μl HCOOH.

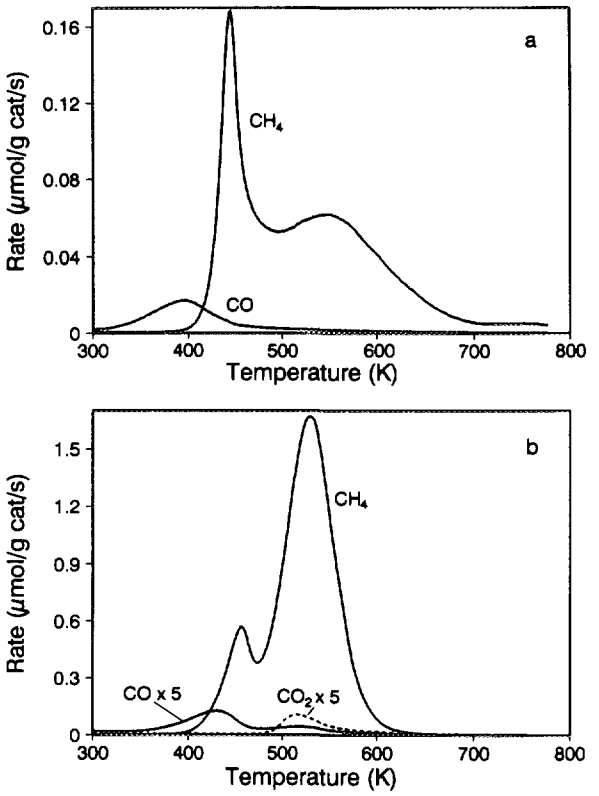

FIG. 5. TPR spectra on 5.7% Ni/Al_2O_3 following CO adsorption (a) in He flow at 300 K for 30 min, (b) in H_2 flow at 385 K for 30 min.

Formic acid also readily adsorbed on the Al_2O_3 surface, and it decomposed much more rapidly than CH_3OH, but its main reaction pathway was dehydration to CO and H_2O (Fig. 4b). Note that the amounts of CO_2 and H_2 are quite small. When 3 μL HCOOH (780 μmol/g catalyst) was adsorbed, 643 μmol CO and 568 μmol H_2O/g catalyst were observed, and the H_2O desorption was not complete when heating was stopped.

Nickel/Alumina

Carbon monoxide hydrogenation. As reported previously (6), CO adsorbed at 300 K on Ni/Al_2O_3 catalysts hydrogenates to CH_4 in two distinct peaks during TPR. As shown in Fig. 5a, the same behavior was observed for the 5.7% Ni/Al_2O_3 catalyst used in this study. The narrow CH_4 peak at 445 K is due to hydrogenation of CO adsorbed on Ni. During TPR, CH_3O forms because of a spillover process, and the CH_4 peak at 546 K results as this CH_3O is hydrogenated. Higher coverage of CH_3O was obtained by CO and H_2 coadsorption at 385 K. For 30 min of coadsorption at 385 K, nine times as much CH_4 formed during the subsequent TPR, and as shown in Fig. 5b, most of the CH_4 formed in the high temperature peak. This 30-

min exposure did not saturate the Al_2O_3 surface, and a much longer exposure time is required for saturation of this low dispersion catalyst.

Methanol hydrogenation. In contrast to adsorbed CO, adsorbed CH_3OH was hydrogenated to CH_4 in a single peak on Ni/Al_2O_3. For an exposure of 25 μmol CH_3OH/g catalyst, the single CH_4 peak was at 532 K; this is almost identical to the CH_4 peak that formed at 530 K (Fig. 5b) from CO and H_2 coadsorption. As shown in Fig. 6a, at higher CH_3OH exposures (500 μmol CH_3OH/g catalyst), CH_4 also formed in a single peak, but the peak temperature increased to 543 K and the peak was narrower (halfwidth of 44 K instead of 58 K). Most of the CH_3OH was hydrogenated to CH_4 (374 μmol/g catalyst), but small amounts of $(CH_3)_2O$ and CO also formed at the same temperature. Even smaller amounts of CO_2 and unreacted CH_3OH were also observed. For higher CH_3OH exposures (750 and 1000 μmol/g catalyst), the size of the CH_4 peak at 543 K increased to 440 and 462 μmol/g catalyst, respectively, but the peak shape was unchanged. As shown in Table 1, the amounts of CO and CH_3OH increased dramatically, while $(CH_3)_2O$ formation increased to a lesser extent.

Of particular significance for CH_3OH hydrogenation is that a low temperature CH_4 peak was *not* observed during TPR. That is, CH_3OH adsorbed at 300 K on Ni/Al_2O_3 did not form CO on Ni, even though CH_3OH adsorbed at 170 K on Ni in UHV forms CO upon decomposition below room temperature (35). Coadsorption of ^{13}CO and CH_3OH at 300 K showed that CO adsorbs on Ni and CH_3OH adsorbs on Al_2O_3 and the two adsorption processes are independent. When ^{13}CO was adsorbed first to saturate the Ni sites, and the catalyst was then exposed to 500 μmol CH_3OH/g catalyst, the $^{13}CH_4$ and $^{12}CH_4$ peaks observed during TPR were the same as the CH_4 peaks in Figs. 5a and 6a, respectively. Similarly, when the adsorption order was reversed, but only 25 μmol CH_3OH/g catalyst was adsorbed, the resulting TPR spectra in Fig. 7 were the same as those seen for individual CO and CH_3OH adsorptions. As observed on the Ni/SiO_2 catalyst, there was no indication that CO displaced adsorbed CH_3OH or vice versa.

TABLE 1

TPR of CH_3OH on Ni/Al_2O_3

CH_3OH exposure (μl)	Amount of products (μmol/g catalyst)				CH_4 peak temperature (K)
	CH_4	CO	CH_3OH	$(CH_3)_2O$	
0.1	21	2	—	—	532
2	374	15	1.4	16	543
3	440	82	17	43	542
4	462	106	156	30	543

Ethanol and 1-propanol hydrogenation. The CH_4 TPR spectra of C_2H_5OH and 1-C_3H_7OH were almost identical to the CH_4 TPR spectrum of CH_3OH. Methane formed in a single peak and essentially the same peak temperatures and peak shapes were obtained. The CH_4 peak from C_2H_5OH hydrogenation, shown in Fig. 6b, has a maximum at 544 K. The large amount of CH_4 formed (685 μmol/g catalyst) following exposure of 340 μmol

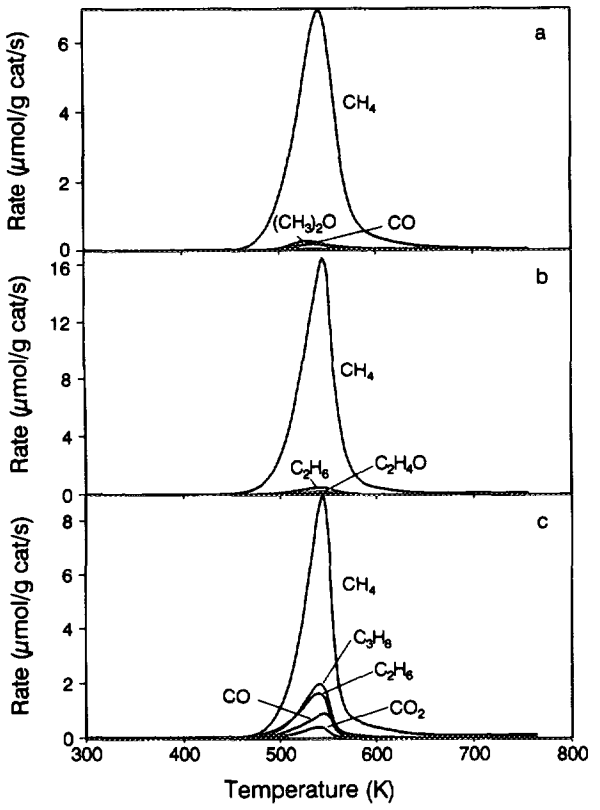

FIG. 6. TPR spectra on 5.7% Ni/Al_2O_3 following adsorption at 300 K of 2 μl of (a) CH_3OH (b) C_2H_5OH, (c) 1-C_3H_7OH.

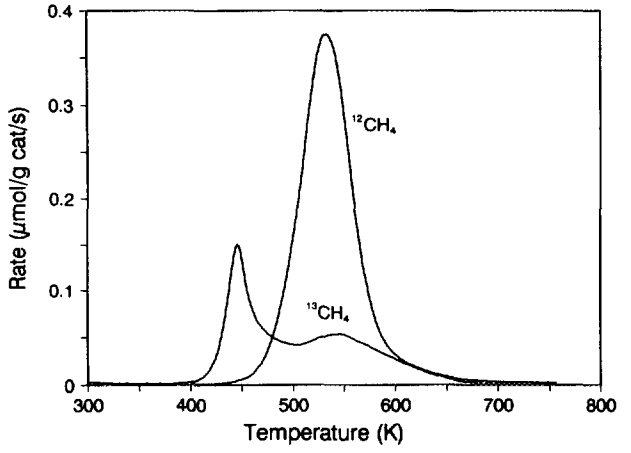

FIG. 7. TPR spectra on 5.7% Ni/Al_2O_3 for 0.1 μl of CH_3OH exposure in He at 300 K followed by ^{13}CO adsorption in He at 300 K for 15 min.

C_2H_5OH/g catalyst indicates that both carbon atoms in C_2H_5OH were hydrogenated to CH_4 in the single peak. Only small amounts of C_2H_6 and C_2H_4O formed, and at the same temperature as CH_4. No unreacted C_2H_5OH was observed. For low C_2H_5OH exposures (17 μmol/g catalyst), the CH_4 peak was similar in shape to that in Fig. 6b, but its peak maximum was 8 K lower.

At high 1-C_3H_7OH exposures (270 μmol/g catalyst), the CH_4 peak temperature was 545 K, and 353 μmol CH_4/g catalyst formed. As shown in Fig. 6c, significant amounts of C_3H_8, C_2H_6, CO, and CO_2 formed at the same temperature as CH_4. At low 1-C_3H_7OH exposures (13.5 μmol/g catalyst), the CH_4 peak shape was the same, but its peak maximum was 9 K lower, and 18 μmol CH_4/g catalyst formed. Over the same temperature range, C_3H_8, CO, C_2H_6, and CO_2 also formed in smaller amounts.

Dimethyl ether and acetone hydrogenation. The CH_4 TPR spectrum for CH_4 formation from adsorbed $(CH_3)_2O$ is almost identical to that for TPR of CH_3OH. As shown in Fig. 8a, CH_4 formed in a single peak centered at 546 K, and more than half the adsorbed $(CH_3)_2O$ desorbed unreacted between 300 and 550 K. A total of 199 μmol CH_4/g catalyst formed. The TPR of $(CH_3)_2O$ to form CH_4 is expected to be similar to TPR of CH_3OH since their TPD spectra from Al_2O_3 are essentially identical. They apparently form the same adsorbed species.

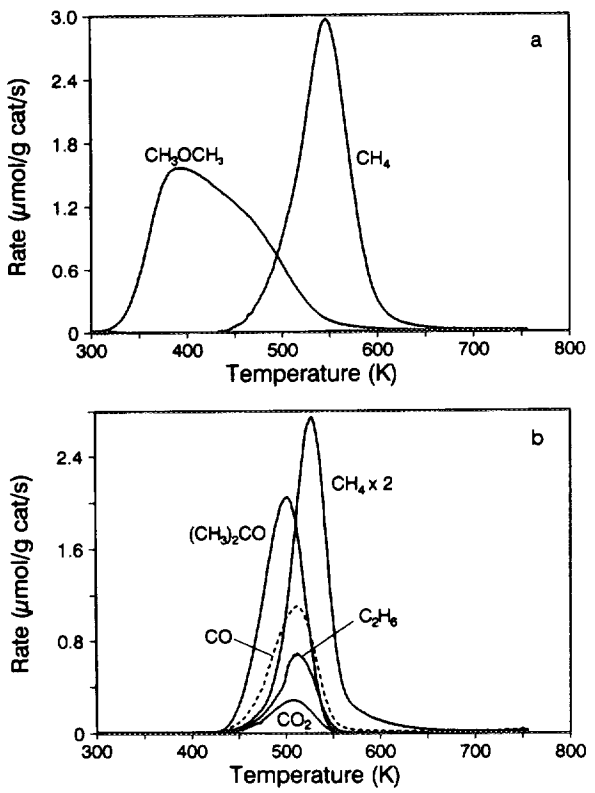

FIG. 8. TPR spectra on 5.7% Ni/Al_2O_3 following adsorption at 300 K of (a) $(CH_3)_2O$ for 15 min, (b) 1 μl $(CH_3)_2CO$.

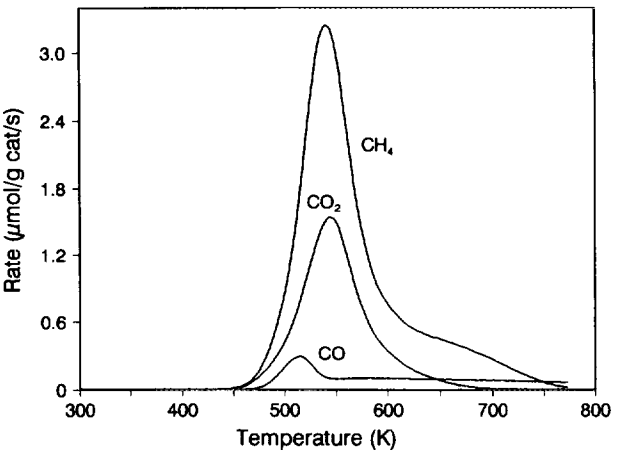

FIG. 9. TPR spectra on 5.7% Ni/Al_2O_3 following 2 μl of HCOOH adsorption in He at 300 K.

Acetone also hydrogenated to CH_4 in a single peak during TPR in a shape that was similar to that obtained for CH_3OH hydrogenation. Two differences were noted, however. The CH_4 peak temperature was 528 K for $(CH_3)_2CO$ hydrogenation, and at high exposures (135 μmol/g catalyst), the dominant species was unreacted $(CH_3)_2CO$, as shown in Fig. 8b. In addition, significant amounts of CO, C_2H_6, and CO_2 formed, but there was no indication that CO was adsorbed on Ni following $(CH_3)_2CO$ adsorption. Similar results were obtained at low $(CH_3)_2CO$ exposures (13.5 μmol/g catalyst); the CH_4 peak temperature and shape were unchanged, and the amount of unreacted $(CH_3)_2CO$ was slightly smaller than the CH_4 amount.

Formic acid hydrogenation. At high exposure (520 μmol/g catalyst), the CH_4 signal during TPR of adsorbed HCOOH was similar to that observed for CH_3OH hydrogenation, and 264 μmol CH_4/g catalyst formed. The peak temperature was 540 K, but as shown in Fig. 9, a high temperature tail extended to 750 K. In addition, CO_2 formed over the same temperature range as CH_4, and the CO_2 amount was 40% of the CH_4 amount. No unreacted HCOOH was observed and only a small amount of CO was seen. At low HCOOH exposure (26 μmol/g catalyst) the CH_4 peak was much broader and the peak temperature was 527 K. The amount of CO_2 formed was insignificant. The high temperature tail for CH_4 at both exposures may be due to hydrogenation of CO_2, which formed from HCOOH decomposition and then readsorbed on the Al_2O_3 surface. When TPR was carried out following CO_2 adsorption at 300 K, the CH_4 peak shape was similar to that observed for low HCOOH exposures. The peak maximum was at 523 K, and CH_4 also formed in a high temperature tail.

Adsorption of ^{13}CO to saturation at 300 K prior to HCOOH adsorption (520 μmol/g catalyst) showed that coadsorbed ^{13}CO was not displaced by HCOOH, nor did it

affect HCOOH adsorption or hydrogenation. The $^{12}CH_4$, $^{12}CO_2$, and ^{12}CO peak shapes and amounts were the same as in Fig. 9. Similarly, the $^{13}CH_4$ and ^{13}CO peak shapes and amounts were the same as those obtained when CO was adsorbed alone (Fig. 5a).

Acetaldehyde hydrogenation. Hydrogenation of C_2H_4O during TPR was only similar to CH_3OH hydrogenation at low exposures. As shown in Fig. 10a, two distinct CH_4 peaks were observed at low exposures (90 μmol/g catalyst). The peak at 539 K was identical in shape, up to approximately 560 K, to the CH_4 peak from hydrogenation of CH_3OH at high coverage, but the high temperature peak was not seen during CH_3OH hydrogenation. In addition to CH_4, C_2H_6 and unreacted C_2H_4O were observed at the same time as the low temperature CH_4 peak.

The TPR spectra changed dramatically at high C_2H_4O exposures (900 μmol/g catalyst), as shown in Fig. 10b. The initial rate of CH_4 formation was slower and CH_4 formed over a broad temperature range in overlapping peaks. This CH_4 signal was unlike that observed for any of the other organics studied. A total of 1050 μmol CH_4/g catalyst formed. In addition, unreacted C_2H_4O started desorbing at 325 K, and C_2H_6 was observed over a broad temperature range. Some C_2H_4O was also hydrogenated to C_2H_5OH at low temperatures.

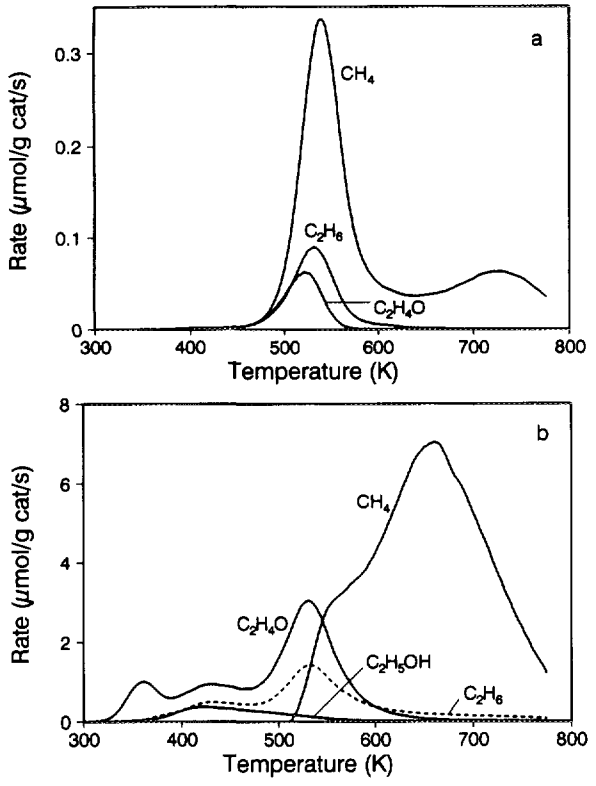

FIG. 10. TPR spectra on 5.7% Ni/Al_2O_3 following C_2H_4O adsorption at 300 K: (a) 0.5 μl, (b) 5 μl.

DISCUSSION

Adsorption Sites

On both Ni/SiO_2 and Ni/Al_2O_3, the organic molecules adsorb directly on the oxide support at 300 K, and they do not adsorb and decompose on the Ni surfaces of the catalysts. The following observations support this conclusion:

- The same amount of oxygenate adsorbed on Al_2O_3 as on Ni/Al_2O_3.
- The amounts adsorbed on Ni/Al_2O_3 are much larger than the amount of CO that can adsorb on the Ni.
- Adsorption amounts differ by more than a factor of 10 between Ni/SiO_2 and Ni/Al_2O_3.
- Preadsorption of CO did not affect adsorption of organics and preadsorption of organics did not affect adsorption of CO on Ni/SiO_2 or Ni/Al_2O_3. That is, the same amount of $^{12}CH_4$ was seen during TPR whether ^{12}C-labeled oxygenate was adsorbed before or after ^{13}CO adsorption. Similarly, the same amount of $^{13}CH_4$ was seen.
- A CH_4 peak corresponding to CO or carbon hydrogenation was not observed during TPR of organic oxygenates; that is, the organics did not adsorb and decompose on the Ni surface of Ni/SiO_2 or Ni/Al_2O_3.

The only exception to these observations is HCOOH adsorption on Ni/SiO_2, and this will be discussed later.

The concentration of adsorption sites on Al_2O_3 is more than an order of magnitude larger than on SiO_2. In addition, CO and H_2 interact on Ni/Al_2O_3 to form CH_3O, which is adsorbed on the support. In contrast, CH_3O did not form on Ni/SiO_2 from CO and H_2 (32), even though CH_3OH adsorbs on Ni/SiO_2. Perhaps the rate of CH_3O formation is much slower from CO and H_2 on Ni/SiO_2, since IR and NMR studies showed that CH_3O and C_2H_5O formed on Rh/SiO_2 at high pressures (15 atm) and temperatures (473 K) (36). Similar conditions were not tried for Ni/SiO_2.

It is surprising that the organic molecules did not adsorb and decompose on the Ni surfaces of Ni/SiO_2 or Ni/Al_2O_3 at room temperature, since some of them adsorb and decompose to adsorbed CO and H below room temperature on single crystal Ni in UHV (37–41). On Ni(111) and Ni(110), for example, CH_3OH formed CH_3O, which decomposed at 290 K or above to form adsorbed CO and H. Most likely, the adsorbed CH_3O and H recombine at room temperature and desorb in our studies. Methanol desorbs near 290 K from Ni(111) due to recombination (41), and CH_3O on Ni(111) was hydrogenated to CH_3OH near 310 K when gas phase H_2 (pressure = 0.02–2.0 Torr) was present (42). Since we use much higher H_2 pressure at room temperature, alcohol molecules adsorbed on the Ni surface can apparently be hydrogenated. Similar processes may occur for the other organics.

Only for formic acid adsorption on Ni/SiO_2 did we see a CH_4 peak during TPR that was the same as CH_4 from CO hydrogenation. As reported previously (43), HCOOH adsorption on SiO_2 is small relative to adsorption on Ni/SiO_2, apparently because the HCOOH mostly adsorbs on the Ni surface. Formic acid decomposition on Ni/SiO_2 forms CO_2, CO, H_2, and H_2O (43, 44). The CO_2 peak at 417 K corresponds to HCOOH decomposition and is similar to that reported previously during TPD (43). The simultaneous formation of H_2 could not be observed because of the H_2 flow. The additional CO_2 and CO that formed at higher temperatures during TPD were hydrogenated to CH_4 during our TPR experiments (Fig. 3). The HCOOH desorption between 300 and 500 K may be from physically adsorbed HCOOH (45, 46).

What is surprising is that HCOOH adsorbed on Ni/Al_2O_3 did not form CO_2 and CO at low temperature, and a CH_4 peak that corresponds to CO hydrogenation was not observed. During TPD of HCOOH adsorbed on Ni/Al_2O_3, products (CO, CO_2, and H_2) started desorbing at 450 K and had maxima at 515 K (47). Apparently HCOOH adsorbed on Ni was able to spill over to the Al_2O_3 surface before it decomposed or was hydrogenated.

Hydrogenation on Nickel/Silica

Figures 1b and 2a show that CH_3OH and C_2H_5OH hydrogenate to CH_4 by similar pathways. In both cases, CH_4 forms in a narrow peak at 495 K and in a broad peak up to 700 K, where the rates start to increase. The TPR experiments with ^{13}CO clearly show that (1) the ^{13}CO adsorbed on Ni did not affect CH_3OH hydrogenation, (2) ^{13}CO hydrogenates faster than CH_3OH or C_2H_5OH, and (3) the hydrogenation behavior of CO is distinctly different from that of the alcohols on Ni/SiO_2. Thus, the alcohols do not decompose on the Ni surface below 450 K to form H and CO (or carbon), which would then be hydrogenated to CH_4.

Alkoxides formation on SiO_2 surfaces from alcohols has been detected in previous studies. Infrared studies of SiO_2 and Rh/SiO_2 showed that CH_3OH formed CH_3O and C_2H_5OH formed C_2H_5O (48–53). Since the alcohols adsorb on SiO_2 to form alkoxides but H_2 adsorbs and dissociates on the Ni surface, a spillover process must be involved in CH_4 formation. For example, the alcohols or alkoxides could diffuse to the $Ni–SiO_2$ interface and be hydrogenated to CH_4. Because some CH_4 forms at high temperatures, this diffusion process does not appear to be fast on SiO_2, and this may be why CH_3O does not readily form from CO and H_2 at 395 K in Ni/SiO_2. Since the TPR spectrum for CH_4 was similar for CH_3OH and $(CH_3)_2CO$, the same type of process may take place during $(CH_3)_2CO$ hydrogenation.

Hydrogenation on Nickel/Alumina

As shown in Table 2, CH_4 peak temperatures are almost identical during TPR of various oxygenates adsorbed on Ni/Al_2O_3. The same peak temperatures mean specific rates of reaction are the same, and thus the same rate-determining step limited CH_4 formation for each adsorbate. None of these adsorbates formed a CH_4 peak that corresponds to hydrogenation of CO adsorbed on Ni. That is, CO was not present on the Ni surface below 450 K, since CH_4 only started to form from these oxygenates above 450 K.

One possible reaction sequence for hydrogenation of these organic oxygenates during TPR is:

H_2 adsorption on Ni:

$$H_2(g) + 2\ S_{Ni} \rightarrow 2\ H–S_{Ni} \quad [1]$$

H atom spillover to the interface:

$$H–S_{Ni} + S_{Ni-Al} \rightarrow H–S_{Ni-Al} + S_{Ni} \quad [2]$$

Oxygenate spillover to the interface:

$$Oxy–S_{Al} + S_{Ni-Al} \rightarrow Oxy–S_{Ni-Al} + S_{Al} \quad [3]$$

Surface reaction:

$$Oxy–S_{Ni-Al} + n\ H–S_{Ni-Al} \rightarrow CH_4(g) + (n + 1)\ S_{Ni-Al} + H_2O(g). \quad [4]$$

Note that reaction [4] is not balanced because $Oxy–S_{Ni-Al}$ denotes various organic oxygenates. This reaction sequence assumes that CH_4 is not adsorbed on the surface. It also assumes that the surface reaction (reaction [4]) takes place at the $Ni–Al_2O_3$ interface, but instead H could spill over and react on the Al_2O_3 or the organic could spill over and react on the Ni. The oxygenates may all

TABLE 2

Methane Peak Temperatures during TPR of Various Oxygenates Adsorbed on Ni/Al_2O_3

Adsorbate	Peak temperature (K)	
	Low coverage	High coverage
CH_3O from CO + H_2	530	—
CH_3OH	532	543
$(CH_3)_2O$	536	546
C_2H_5OH	536	544
1-C_3H_7OH	536	545
HCOOH	527	540
$(CH_3)_2CO$	528	528
C_2H_4O	539	660
CO	445	455

decompose to CO and CH_x before hydrogenation since the subsequent hydrogenation of these species would be fast, and thus reaction [4] may be a series of steps. Deuterium isotope labeling experiments on Ni/Al_2O_3 (54) showed that gas-phase H_2 undergoes spillover from Ni to Al_2O_3 and exchange with CH_3OD adsorbed on Al_2O_3 at a faster rate than CH_3O decomposition or hydrogenation. Thus, H_2 adsorption is not rate limiting. If the H spillover processes for exchange and hydrogenation are similar, then H spillover does not appear to be rate-limiting for organic oxygenates hydrogenation on Ni/Al_2O_3. Because TPD experiments show that CH_3OH, C_2H_5OH, and 1-C_3H_7OH all decompose at similar rates and since this decomposition appears to occur by reverse spillover to the $Ni–Al_2O_3$ interface (34), a likely rate-limiting step for CH_4 formation is reaction [3], the reverse spillover step. Further support for this conclusion is the fact that alcohol decomposition during TPD has a maximum at a similar temperature to CH_4 formation during TPR. The CH_4 peak starts to form at a higher temperature and CH_4 formation is complete at a lower temperature during TPR than the CO and H_2 from decomposition during TPD. Since hydrogen is a product of oxygenate decomposition, it may inhibit decomposition when present at ambient pressure and thus delay the decomposition and subsequent hydrogenation (33).

As oxygenate coverage increased, the CH_4 peak temperature also increased for most adsorbates used. That is, the hydrogenation appears to be less than first order in oxygenate coverage. If reaction occurs at the $Ni–Al_2O_3$ interface, increasing the coverage on the Al_2O_3 will not necessarily increase the rate because the sites at the interface may become saturated. Higher temperatures are then required to increase the reaction rate at the interface.

Although CH_4 forms at essentially the same rate during TPR for all the oxygenates studied, the adsorbed intermediate is probably not the same. If the rate of reverse spillover is independent of the adsorbed species, then the rate of hydrogenation could be the same for the various oxygenates. Because of the different types of adsorbates used, it is difficult to envision a common intermediate. In addition, parallel reactions occur for many of the intermediates. For example, $(CH_3)_2CO$, C_2H_6, CO_2, and CO formed in significant quantities during TPR of adsorbed $(CH_3)_2CO$. At high coverages, $(CH_3)_2CO$ was the dominant species, and CO was almost as large as CH_4. In contrast, for some of the other species (CH_3O, CH_3OH, $(CH_3)_2O$), methane was found almost exclusively.

Similarly, at low coverages, C_2H_4O hydrogenated to CH_4 at the same rate as the other oxygenates, but as shown in Fig. 10b, the CH_4 TPR spectrum was quite different at high coverages. The CH_4 peak extended to 773 K, with a maximum above 650 K. Apparently some adsorbed species could not reach the $Ni–Al_2O_3$ interface before a parallel reaction took place to form species that were less readily hydrogenated to CH_4. The lower reactivity of C_2H_4O is also reflected in its TPD spectra. The CO and CO_2 products from C_2H_4O did not start to appear until 650 K (47), but the products from TPD of C_2H_5OH form between 400 and 900 K (34). The high temperature CH_4 peak may be due to hydrogenation of acetate that formed from C_2H_4O, since the CH_4 peak location was similar to the high temperature tail from formate hydrogenation in Fig. 9. Also, IR studies (55, 56) showed that C_2H_4O adsorbed on Al_2O_3 to form acetate above 473 K. Formic acid hydrogenation also exhibited differences from the other oxygenates. At low coverage, HCOOH hydrogenated to CH_4 in a broad peak that extended above 750 K. This may also reflect parallel decomposition to form CO_2 and H_2. The CO_2 readily adsorbs on Al_2O_3 and may be responsible for the high temperature tail since CO_2 adsorbed on Al_2O_3 hydrogenates to CH_4 in a similar matter to HCOOH (a similar peak temperature and a broad high temperature tail). Moreover, the high temperature tail was not observed for HCOOH on Ni/SiO_2, and CO_2 does not adsorb on SiO_2.

CONCLUSIONS

A series of organic oxygenates exhibits similar behavior on supported nickel catalysts. The oxygenates readily adsorb on the Al_2O_3 surface of Ni/Al_2O_3. They do not strongly adsorb on Ni and are easily hydrogenated or they readily spill over from Ni to Al_2O_3. Thus, none of the oxygenates studied (CH_3OH, C_2H_5OH, 1-C_3H_7OH, C_2H_4O, $(CH_3)_2O$, HCOOH, $(CH_3)_2CO$) dissociates on the Ni surface of Ni/Al_2O_3 to form CO. The rates of hydrogenation to CH_4 are essentially the same for all the oxygenates studied, although HCOOH and C_2H_4O exhibit differences at low/high coverages. Hydrogenation involves a spillover process, since H_2 dissociates on the Ni surface but the organics are adsorbed on the Al_2O_3 surface. The same rate-determining step, reverse spillover of the organic from Al_2O_3 to Ni, appears to limit the formation of CH_4. Carbon monoxide adsorbed on Ni does not affect organic adsorption or hydrogenation, nor is its adsorption or hydrogenation affected by adsorbed organics. Adsorbed CH_3O, formed by CO and H_2 coadsorption at elevated temperatures, exhibits the same hydrogenation behavior as adsorbed CH_3OH. Similar processes appear to take place on Ni/SiO_2 for adsorbed CH_3OH and C_2H_5OH, but the surface coverages on SiO_2 are a factor of 15 smaller and the processes are slower. In addition, HCOOH dissociates on the Ni surface to form CO and CO_2.

ACKNOWLEDGMENT

We gratefully acknowledge support by the National Science Foundation, Grant CTS-9021194.

REFERENCES

1. Ozdogan, S. Z., Gochis, P. D., and Falconer, J. L., *J. Catal.* **83,** 257 (1983).
2. Kester, K. B., and Falconer, J. L., *J. Catal.* **89,** 380 (1984).
3. Kester, K. B., Zagli, E., and Falconer, J. L., *Appl. Catal.* **22,** 311 (1986).
4. Huang, Y. J., and Schwarz, J. A., *Appl. Catal.* **24,** 241 (1986).
5. Bailey, K. M., Chai, G. Y., and Falconer, J. L., "Proceedings, 9th International Congress on Catalysis, Calgary, 1988" (M. J. Phillips and M. Ternan, Eds.), Vol. 3, p. 1090. Chem. Institute of Canada, Ottawa, 1988.
6. Glugla, P. G., Bailey, K. M., and Falconer, J. L., *J. Phys. Chem.* **92,** 4474 (1988).
7. Chen, B., Falconer, J. L., and Chang, L., *J. Catal.* **127,** 732 (1991).
8. Greenler, R. G., *J. Chem. Phys.* **37,** 2094 (1962).
9. Rossi, P. F., Busca, G., and Lorenzelli, V., *Z. Phys. Chem.* **149,** 99 (1986).
10. Busca, G., Rossi, P. F., and Lorenzelli, V., *J. Phys. Chem.* **89,** 5433 (1985).
11. Arai, H., Saito, Y., and Yoneda, Y., *Bull. Chem. Soc. Jpn.* **40,** 731 (1967).
12. Deo, A. V., and Dalla Lana, I. G., *J. Phys. Chem.* **73,** 716 (1969).
13. Kagel, R. O., *J. Phys. Chem.* **71,** 844 (1967).
14. Palazov, A., Kadinov, G., Boner, C., and Shapov, D., *J. Catal.* **74,** 44 (1982).
15. Lü, Y., Xue, J., Li, X., Fu, G., and Zhang, D., *Cuihua Xuebao* **6,** 116 (1985).
16. Mirodatos, C., Prauliaud, H., and Primet, M., *J. Catal.* **107,** 275 (1987).
17. Della-Betta, R. A., and Shelef, M., *J. Catal.* **48,** 111 (1977).
18. Hirota, K., Fueki, K., Shindo, K., and Nakai, Y., *Bull. Chem. Soc. Jpn.* **32,** 1261 (1959).
19. Amenomiya, Y., *Appl. Spectrosc.* **32,** 484 (1978).
20. Amenomiya, Y., *J. Catal.* **57,** 64 (1979).
21. Solymosi, F., Bánsági, T., and Erdöhelyi, A., *J. Catal.* **72,** 166 (1981).
22. Matsushima, T., and White, J. M., *J. Catal.* **44,** 183 (1976).
23. DeCanio, E. C., Nero, V. P., and Bruno, J. W., *J. Catal.* **135,** 444 (1992).
24. Chen, J. G., Basu, P., Ballinger, T. H., and Yates, J. T., Jr., *Langmuir* **5,** 352 (1989).
25. Hindermann, J. P., Deluzarche, A., Kieffer, R., and Kiennemann, A., *Can. J. Chem. Eng.* **61,** 21 (1983).
26. Robbins, J. L., and Maruchi-Soos, E., *J. Phys. Chem.* **93,** 2885 (1989).
27. Vannice, M. A., and Twu, C. C., *J. Catal.* **82,** 213 (1983).
28. Vannice, M. A., and Sudhakar, C., *J. Phys. Chem.* **88,** 2429 (1984).
29. Sen, B., and Vannice, M. A., *J. Catal.* **113,** 52 (1988).
30. Swecker, J. L., and Datye, A. K., *J. Catal.* **121,** 196 (1990).
31. Sen, B., Falconer, J. L., Mao, T., Yu, M., and Flesner, R. L., *J. Catal.* **126,** 465 (1990).
32. Sen, B., and Falconer, J. L., *J. Catal.* **117,** 404 (1989).
33. Sen, B., and Falconer, J. L., *J. Catal.* **125,** 35 (1990).
34. Chen, B., and Falconer, J. L., *J. Catal.* **144,** 214 (1993).
35. Richter, L. J., Gurney, B. A., Villarrubia, J. S., and Ho, W., *Chem. Phys. Lett.* **11,** 185 (1984).
36. Chudek, J. A., McQuire, M. W., and Rochester, C. H., *J. Catal.* **135,** 358 (1992).
37. Demuth, J. E., and Ibach, H., *Chem. Phys. Lett.* **60,** 395 (1979).
38. Rubloff, G. W., and Demuth, J. E., *J. Vac. Sci. Technol.* **14,** 419 (1977).
39. Erskine, J. L., and Bradshaw, A. M., *Chem. Phys. Lett.* **72,** 260 (1980).
40. Gates, S. M., Russell, J. N., Jr., and Yates, J. T., Jr., *Surf. Sci.* **146,** 199 (1984).
41. Gates, S. M., Russell, J. N., Jr., and Yates, J. T., Jr., *Surf. Sci.* **159,** 233 (1985).
42. Zhang, R., and Gellman, A. J., *Catal. Lett.*, in press.
43. Falconer, J. L., Burger, L. C., Corfa, I. P., and Wilson, K. G., *J. Catal.* **104,** 424 (1987).
44. Iglesia, E., and Boudart, M., *J. Catal.* **81,** 224 (1981).
45. Li, G., Ridd, M. J., and Larkins, F. P., *Aust. J. Chem.* **44,** 623 (1991).
46. Solymosi, F., Erdöhelyi, A., and Bánsági, T., *J. Chem. Soc., Faraday Trans. 1* **77,** 2645 (1981).
47. Chen, B., Ph.D. Dissertation, Department of Chemical Engineering, University of Colorado, 1993.
48. Borello, E., Zecchina, A., and Morterra, C., *J. Phys. Chem.* **71,** 2938 (1967).
49. Morrow, B. A., *J. Chem. Soc., Faraday Trans. 1* **70,** 1527 (1974).
50. Monti, D. M., Cant, N. W., Trimm, D. L., and Wainwright, M. S., *J. Catal.* **100,** 17 (1986).
51. Lavalley, J. C., Saussey, J., Lamotte, J., Breault, R. Hindermann, J. P., and Kiennemann, A., *J. Phys. Chem.* **94,** 5941 (1990).
52. Anderson, J. A., McQuire, M. W., Rochester, C. H., and Sweeney, T., *Catal. Today* **9,** 29 (1991).
53. McQuire, M. W., Rochester, C. H., and Anderson, J. A., *J. Chem. Soc., Faraday Trans. 1* **87,** 1921 (1991).
54. Flesner, R. L., and Falconer, J. L., submitted for publication.
55. Fink, P., *Z. Chem.* **7,** 284 (1967).
56. Fink, P., *Rev. Roum. Chim.* **14,** 811 (1969).